Templated Fabrication of Periodic Metallic Nanopyramid Arrays

Chih-Hung Sun, Nicholas C. Linn, and Peng Jiang*

Department of Chemical Engineering, University of Florida, Gainesville, Florida 32611

Received May 7, 2007. Revised Manuscript Received June 22, 2007

This paper reports a simple self-assembly-based templating approach for fabricating wafer-scale, periodic metallic nanopyramid arrays with nanoscale tips and high tip density (6×10^8 tips cm^{-2}). Spin-coated, non-close-packed monolayer colloidal crystals are used as templates to create chromium nanohole arrays, which are utilized as etching masks to fabricate inverted silicon pyramidal pits by anisotropic KOH etching. Wafer-scale metallic pyramid arrays with sharp nanotips can then be replicated from silicon templates by a simple adhesive peeling process. This nonlithographic technique combines the simplicity and cost benefits of bottom-up self-assembly with the scalability and compatibility of standard top-down microfabrication in creating periodic metallic nanostructures that are not easily available by conventional nanofabrication. The resulting nanopyramid arrays show stable surface enhancements for Raman scattering from benzenethiol molecules adsorbed at the metal surfaces, even though these sputtered films are not rough.

Introduction

Metallic substrates with periodic subwavelength structures exhibit unique surface plasmon properties that are of great scientific interest and considerable technological importance in developing nanophotonic devices, data storage, and biosensors.[1−6] Metallic nanotips are particularly interesting as surface-enhanced Raman scattering (SERS) substrates because they can concentrate electromagnetic field at the tip apex, resulting in a great enhancement of the Raman scattering intensity from molecules in the vicinity of the nanoscopic tips.[7−10] Scanning probe microscopy (SPM) tips coated with noble metals (e.g., Au and Ag) have been shown to enhance Raman scattering by 3−6 orders of magnitude.[9,10] The Raman enhancement factor of gold nanocrescent moons with sub-10 nm sharp edges, which are templated from sacrificial microspheres, is estimated to be larger than 1×10^{10}, making them promising for ultrasensitive biosensors.[7] Other asymmetric metallic nanostructures, such as half-shells,[11] nanocups,[12] nanoprisms,[13] and nanorings,[14] have also been developed for potential SERS applications. Unfortunately, precise control over the position, orientation, and spacing of these aspheric nanomaterials is not trivial and impedes the experimental reproducibility of SERS sensing.

Planar nanotip arrays with high tip density and aligned tip orientation are promising SERS substrates that could resolve the reproducibility issue of current tip-enhanced Raman spectroscopy.[8] Electron-beam lithography (EBL) and focused ion-beam (FIB) lithography are two popular technologies used to create periodic metallic nanostructures with arbitrary patterns.[15,16] Unfortunately, the high-cost and the low-throughput greatly limit the implementation of these advanced lithographic techniques in practical application. Templated synthesis provides a much cheaper, simpler, and faster alternative to complex nanolithography in creating periodic metallic nanostructures.[17] Examples include an array of metallic pyramids with nanoscale tips made by templated deposition of metals on anisotropically etched silicon pits, which are defined by phase-shifting photolithography,[18−20] and an array of submicrometer-scale particles with uniform periodic spacing and nearly uniform size and crystallographic orientations prepared by solid-state dewetting of gold thin films on oxidized silicon surfaces patterned with pyramidal pits by interference lithography.[21] Other templates, such as block-copolymers,[22] colloids,[23−25] and even biological ma-

* To whom correspondence should be addressed. E-mail: pjiang@che.ufl.edu.

(1) Genet, C.; Ebbesen, T. W. *Nature* **2007**, *445*, 39.
(2) Dieringer, J. A.; McFarland, A. D.; Shah, N. C.; Stuart, D. A.; Whitney, A. V.; Yonzon, C. R.; Young, M. A.; Zhang, X. Y.; Van Duyne, R. P. *Faraday Discuss.* **2006**, *132*, 9.
(3) Baker, G. A.; Moore, D. S. *Anal. Bioanal. Chem.* **2005**, *382*, 1751.
(4) Xia, Y. N.; Halas, N. J. *MRS Bull.* **2005**, *30*, 338.
(5) Barnes, W. L.; Dereux, A.; Ebbesen, T. W. *Nature* **2003**, *424*, 824.
(6) Kneipp, K.; Kneipp, H.; Kneipp, J. *Acc. Chem. Res.* **2006**, *39*, 443.
(7) Lu, Y.; Liu, G. L.; Kim, J.; Mejia, Y. X.; Lee, L. P. *Nano Lett.* **2005**, *5*, 119.
(8) Chattopadhyay, S.; Chen, L. C.; Chen, K. H. *Crit. Rev. Solid State Mater. Sci.* **2006**, *31*, 15.
(9) Watanabe, H.; Ishida, Y.; Hayazawa, N.; Inouye, Y.; Kawata, S. *Phys. Rev. B* **2004**, *69*, 155418.
(10) Pettinger, B.; Ren, B.; Picardi, G.; Schuster, R.; Ertl, G. *Phys. Rev. Lett.* **2004**, *92*, 096101.
(11) Love, J. C.; Gates, B. D.; Wolfe, D. B.; Paul, K. E.; Whitesides, G. M. *Nano Lett.* **2002**, *2*, 891.
(12) Charnay, C.; Lee, A.; Man, S. Q.; Moran, C. E.; Radloff, C.; Bradley, R. K.; Halas, N. J. *J. Phys. Chem. B* **2003**, *107*, 7327.
(13) Jin, R. C.; Cao, Y. C.; Hao, E. C.; Metraux, G. S.; Schatz, G. C.; Mirkin, C. A. *Nature* **2003**, *425*, 487.
(14) Aizpurua, J.; Hanarp, P.; Sutherland, D. S.; Kall, M.; Bryant, G. W.; de Abajo, F. J. G. *Phys. Rev. Lett.* **2003**, *90*, 057401.
(15) Kahl, M.; Voges, E.; Kostrewa, S.; Viets, C.; Hill, W. *Sens. Actuators, A* **1998**, *51*, 285.
(16) Ebbesen, T. W.; Lezec, H. J.; Ghaemi, H. F.; Thio, T.; Wolff, P. A. *Nature* **1998**, *391*, 667.
(17) Ozin, G. A.; Arsenault, A. C. *Nanochemistry: A Chemical Approach to Nanomaterials*; RSC Publishing: Cambridge, U.K., 2005.
(18) Henzie, J.; Barton, J. E.; Stender, C. L.; Odom, T. W. *Acc. Chem. Res.* **2006**, *39*, 249.
(19) Henzie, J.; Kwak, E. S.; Odom, T. W. *Nano Lett.* **2005**, *5*, 1199.
(20) Henzie, J.; Shuford, K. L.; Kwak, E. S.; Schatz, G. C.; Odom, T. W. *J. Phys. Chem. B* **2006**, *110*, 14028.
(21) Giermann, A. L.; Thompson, C. V. *Appl. Phys. Lett.* **2005**, *86*, 121903.

10.1021/cm0712319 CCC: $37.00
Published on Web 08/10/2007

terials,[26] have also been utilized in fabricating periodic metallic nanostructures with length scales ranging from nanometer to micrometer. However, most of these templating approaches either still require some sort of lithographic patterning or are not compatible with standard microfabrication, thereby impeding the cost-efficiency and scale-up of these unconventional methodologies.

We have recently developed a robust spin-coating technological platform that combines the simplicity and cost benefits of bottom-up self-assembly with the scalability and compatibility of standard top-down microfabrication in creating a large variety of nanostructured materials.[27,28] The methodology is based on shear-aligning concentrated colloidal suspensions using standard spin-coating equipment. The shear flow generated during the spin-coating process coupled with interparticle interaction induces the formation of wafer-scale, non-close-packed colloidal crystals with adjustable thickness ranging from monolayer to hundreds of layers.[27,28] We have shown that these self-assembled colloidal arrays can be used as structural templates to make a myriad of metallic nanostructures. For instance, periodic nanohole arrays are templated against two-dimensional (2D) non-close-packed colloidal crystals by depositing metals in the interstitials, followed by lifting off colloidal particles.[29] These metallic nanohole arrays can be used as second-generation etching masks during anisotropic reactive ion etching (RIE) to define nanopillar arrays in the substrate.[29] Metallic gratings with crystalline arrays of voids are replicated on the outer surface of three-dimensional (3D) non-close-packed colloidal crystals.[30] Magnetic nanodot arrays can be templated from sacrificial polymer microwell arrays by masked evaporation and polymer liftoff.[31]

Here, we extend our previous work on metallic nanohole arrays to develop a new templating technique for fabricating wafer-scale, periodic metallic pyramid arrays with nanoscale tips and high tip density. Instead of using expensive RIE to pattern silicon nanopillars with vertical sidewalls as shown in our previous work,[29] anisotropic KOH wet etching is utilized to transfer the periodic circular nanoholes into inverted pyramid arrays in (100) silicon wafers. These inverted pyramids can then be used as third-generation templates for replicating large-area metallic nanopyramid arrays by simple physical vapor deposition and adhesive peeling. This new nanofabrication approach is based solely on self-assembly and templated fabrication − no lithographic patterning is involved in any step. Yet this technology is still scalable and compatible with standard microfabrication, enabling large-scale production of metallic nanostructures for potential SERS applications. The Raman scattering spectra of benzenethiol molecules adsorbed on the templated gold nanopyramid arrays are characterized, and the Raman enhancement factor is estimated to be around 7×10^5, even though these sputtering-deposited films are not rough.

Experimental Section

Materials and Substrates. All solvents and chemicals are of reagent quality and are used without further purification. Technical-grade KOH flakes and anhydrous 2-propanol are purchased from Fisher Chemicals and Sigma-Aldrich, respectively. Ultrapure water (18.2 MΩ cm^{-1}) is used directly from a Barnstead water system. Benzenethiol (>98% purity) is purchased from Sigma-Aldrich. Monodispersed silica colloids with less than 5% diameter variation are synthesized by the Stober method.[32,33] Ethoxylated trimethylolpropane triacrylate (ETPTA) monomer is obtained from Sartomer (Exton, PA). The photoinitiator, Darocur 1173 (2-hydroxy-2-methyl-1-phenyl-1-propanone), is provided by Ciba Specialty Chemicals. The silicon wafer primer, 3-acryloxypropyl trichlorosilane (APTCS), is purchased from Gelest (Morrisville, PA). Silicon wafers (test grade, n type, (100)) are obtained from Wafernet (San Jose, CA) and primed by swabbing APTCS on the wafer surfaces using cleanroom Q-tips (Fisher), rinsed and wiped with 200 proof ethanol three times, spin coated with a 200 proof ethanol rinse at 3000 rpm for 1 min, and baked on a hot plate at 110 °C for 2 min.

Instrumentation. Scanning electron microscopy is carried out on a JEOL 6335F FEG-SEM. A standard spin coater (WS-400B-6NPP-Lite Spin Processor, Laurell) is used to spin-coat colloidal suspensions. The polymerization of ETPTA monomer is carried out on a Pulsed UV Curing System (RC 742, Xenon). A Unaxis Shuttlelock RIE/ICP reactive-ion etcher is utilized to remove polymerized ETPTA for releasing shear-aligned colloidal crystals. A Kurt J. Lesker CMS-18 Multi-target Sputter is used to deposit metals. Raman spectra are measured with a Renishaw inVia confocal Raman microscope.

Periodic Metallic Nanohole Arrays Templated from Two-Dimensional Non-Close-Packed Colloidal Crystals. The fabrication of wafer-scale, monolayer, non-close-packed colloidal crystal−polymer nanocomposites is performed according to ref 27. In short, monodispersed silica colloids are dispersed in ETPTA to make final particle volume fraction of ~20%; 2 wt % Darocur 1173 is added as photoinitiator. The silica−ETPTA dispersion is dispensed on a 3-acryloxypropyl trichlorosilane (APTCS)-primed (100) silicon wafer and spin-coated at 8000 rpm for 6 min on a standard spin-coater, yielding a hexagonally ordered colloidal monolayer. The monomer is then photopolymerized for 4 s using a Pulsed UV Curing System. The polymer matrix is fully removed using a reactive ion etcher operating at 40 mTorr oxygen pressure, 40 sccm flow rate, and 100 W for 4 min. A 30 nm mask of chromium is deposited on the wafer using sputtering deposition at a deposition rate of 1.6 Å/s. The wafer is then rinsed in deionized water and rubbed with a cleanroom Q-tip to remove templating silica microspheres. Templating silica particles can also be removed by dissolving them in a 2 vol % hydrofluoric acid aqueous solution for 2−3 min. The removal of the particles creates a visible color change.

Anisotropic Wet Etching and Templated Fabrication of Periodic Metallic Nanopyramid Arrays. The (100) silicon wafer covered by arrays of chromium nanoholes is then wet etched in a

(22) Lu, J.; Chamberlin, D.; Rider, D. A.; Liu, M. Z.; Manners, I.; Russell, T. P. *Nanotechnology* **2006**, *17*, 5792.
(23) Jang, S. G.; Yu, H. K.; Choi, D. G.; Yang, S. M. *Chem. Mater.* **2006**, *18*, 6103.
(24) Tessier, P. M.; Velev, O. D.; Kalambur, A. T.; Rabolt, J. F.; Lenhoff, A. M.; Kaler, E. W. *J. Am. Chem. Soc.* **2000**, *122*, 9554.
(25) Mahajan, S.; Abdelsalam, M.; Suguwara, Y.; Cintra, S.; Russell, A.; Baumberg, J.; Bartlett, P. *Phys. Chem. Chem. Phys.* **2007**, *9*, 104.
(26) Payne, E. K.; Rosi, N. L.; Xue, C.; Mirkin, C. A. *Angew. Chem., Int. Ed.* **2005**, *44*, 5064.
(27) Jiang, P.; McFarland, M. J. *J. Am. Chem. Soc.* **2004**, *126*, 13778.
(28) Jiang, P.; Prasad, T.; McFarland, M. J.; Colvin, V. L. *Appl. Phys. Lett.* **2006**, *89*, 011908.
(29) Jiang, P.; McFarland, M. J. *J. Am. Chem. Soc.* **2005**, *127*, 3710.
(30) Jiang, P. *Angew. Chem., Int. Ed.* **2004**, *43*, 5625.
(31) Jiang, P. *Langmuir* **2006**, *22*, 3955.
(32) Stober, W.; Fink, A.; Bohn, E. *J. Colloid Interface Sci.* **1968**, *26*, 62.
(33) Jiang, P.; Bertone, J. F.; Hwang, K. S.; Colvin, V. L. *Chem. Mater.* **1999**, *11*, 2132.

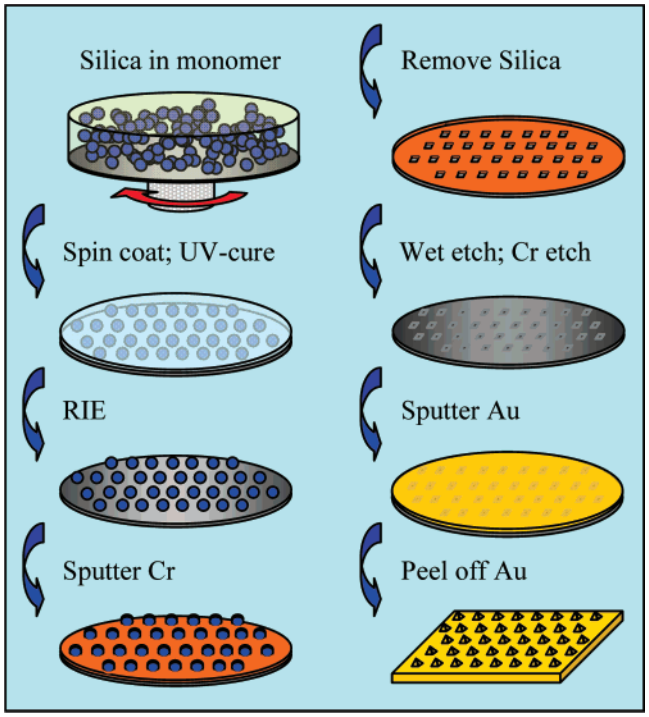

Figure 1. Schematic illustration of the templating procedures for making periodic metallic nanopyramid arrays.

freshly prepared solution of 62.5 g KOH, 50 mL of anhydrous 2-propanol, and 200 mL of ultrapure water at 60 °C for various durations. The wafer is rinsed with deionized water and then wet etched with a chromium etchant (type 1020, Transene) to remove the chromium template. The etched wafers show iridescence under white light illumination. To create a nanopyramid array in gold, we sputtered the wafer with 500 nm of gold at a deposition rate of ~5 Å/s. The layer of gold on the surface of the wafer can be easily peeled off with Scotch tape (3M), yielding a non-close-packed nanopyramid array in gold. To separate the metallic nanopyramid arrays from the silicon templates in a more reliable and reproducible way, we applied a thin layer of polyurethane adhesive (NOA 60, Norland Products) between the metallized wafer and a glass substrate. The adhesive is then polymerized by exposure to ultraviolet radiation. The silicon wafer templates can finally be peeled off, resulting in the formation of wafer-scale nanopyramid arrays supported on glass substrates.

Raman Spectra Measurements. Gold nanopyramid array samples are placed in a 5 mM solution of benzenethiol in 200 proof ethanol for 45 min and then rinsed in roughly 25 mL of 200 proof ethanol for several minutes. The samples are allowed to dry in air for 20 min, after which the Raman spectra are measured. A flat gold film sputtering-deposited on a glass slide using the same deposition condition is used as the control sample for Raman spectra measurements. Raman spectra are measured with a Renishaw inVia confocal Raman microscope using a 785 nm diode laser at 15 mW with an integration time of 10 s and a 40 μm^2 spot size.

Results and Discussion

In contrast with previous lithographic approaches to fabricating nanopyramid arrays,[8,19] our method is simply based on colloidal self-assembly and templated synthesis. A schematic outline of the fabrication procedures is shown in Figure 1. We start from spin-coating concentrated silica−ETPTA monomer dispersions using a standard spin-coater.[27] Wafer-scale, monolayer, hexagonally ordered colloidal arrays

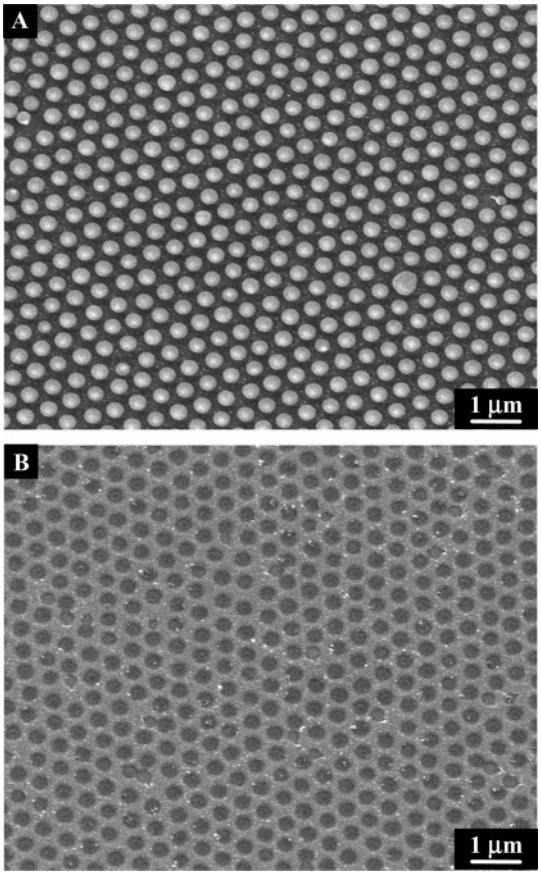

Figure 2. (A) Scanning electron microscope (SEM) image of a spin-coated monolayer non-close-packed colloidal crystal consisting of 320 nm silica spheres. (B) SEM image of a chromium nanohole array templated from the sample shown in (A).

can be reproducibly made in minutes by controlling the spin speed and time.[28] Following a rapid photopolymerization of ETPTA monomer to immobilize silica particles, the polymer matrix is removed by a brief oxygen plasma etch. The resulting colloidal monolayer exhibits non-close-packed arrangement of particles with interparticle distance of ~1.4*D*, where *D* is the diameter of the silica spheres (see Figure 2A). Using this simple spin-coating method, silica particles with a wide range of sizes from ~100 nm to larger than 1 μm have been assembled into monolayer crystals.[27] Manipulation of silica particle size enables control of the size and separation of nanopyramids in the templated arrays.

These shear-aligned, non-close-packed silica particles can then be utilized as deposition masks during conventional physical vapor deposition (e.g., sputtering, thermal evaporation, or electron-beam evaporation).[29] The deposited metals, such as Cr or Ti/Au, fill the interstitials between silica spheres and accumulate on the top halves of particles as well. Because silica particles are loosely attached to the substrate, they can be easily removed by gentle rubbing with a cleanroom swab, leaving behind a metallic nanohole arrays as shown by the SEM image in Figure 2B. Templating silica spheres can also be removed by dissolving in a 2% hydrofluoric acid aqueous solution to lift off metals. We found that a thin layer of chromium (20−30 nm) is sufficient to sustain the KOH wet etching in the following step. These circular nanoholes retain the size and spacing of the templating silica spheres as well as their hexagonal long-

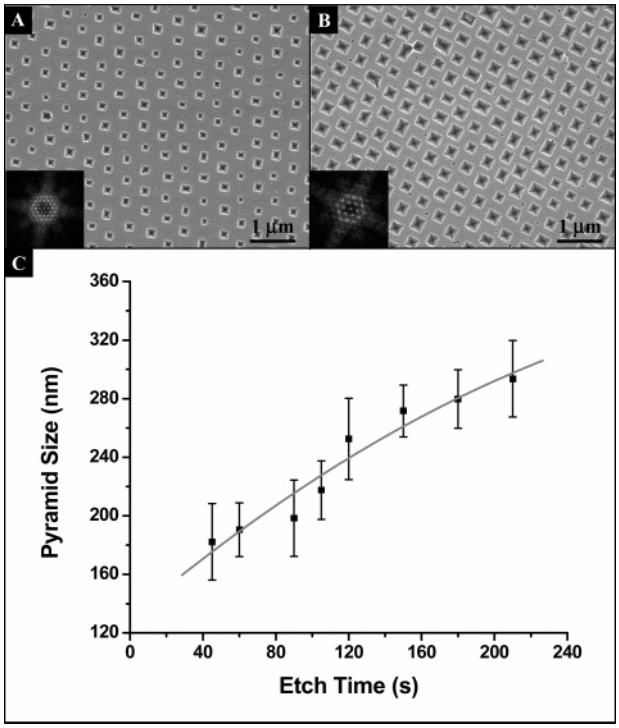

Figure 3. Inverted pyramid arrays anisotropically etched in (100) silicon wafer. (A) SEM image of a sample etched at 60 °C for 120 s. The inset showing a Fourier transform of the image. (B) SEM image of a sample etched at 60 °C for 420 s. The inset showing a Fourier transform of the image. (C) Average size and size distribution of inverted pyramids etched at 60 °C for various durations.

range ordering. Under white light illumination, these templated nanohole arrays function as diffraction gratings, exhibiting strong iridescence.[29] Shape and edge roughness of the templated nanoholes determine the qualities of the resulting inverted pyramids in silicon,[19] thus precautions need to be taken to ensure circular shapes and smooth edges of the metallic nanoholes. Slower PVD deposition rate helps to reduce the grain size and the roughness of edges, whereas thermal or EB evaporation, which is more unidirectional in deposition, is better than sputtering in maintaining the circular shapes of nanoholes.[34]

We then use templated chromium nanohole arrays as second-generation etching masks to create inverted pyramid arrays in (100) silicon wafers through anisotropic etching in an aqueous solution containing KOH and 2-propanol. It is well-known that KOH is a wet etchant that attacks silicon preferentially in the <100> plane, producing characteristic anisotropic V-shape pitches with 54.7° sidewalls.[34] Images A and B in Figure 3 show SEM images of pyramidal pits that are templated from 320 nm silica spheres and etched at 60 °C for 120 and 420 s, respectively. The long-range hexagonal ordering of these pits is obvious from the SEM images and is further confirmed by the hexagonally arranged dots in the fast Fourier transform (FFT) of these images (insets of images A and B in Figure 3). Another interesting feature of the calculated FFTs is the two sets of four-arm stars with exact 90° angles between neighboring arms surrounding the central dots, characteristic of square pyramidal pits. The orthogonal crosses at the centers of the pits also verify the inverted pyramidal structures. The spacing between neighboring pits is the same as that of the original non-close-packed colloidal arrays (Figure 2A), whereas the pit size (252 ± 28 nm) for the 120 s sample is smaller than the size of the nanoholes (~320 nm). This indicates that the etching reaction starts from the center of the nanoholes and then propagates to the edges; otherwise, the spacing between neighboring nanoholes could not be retained in the templated pyramidal pits.

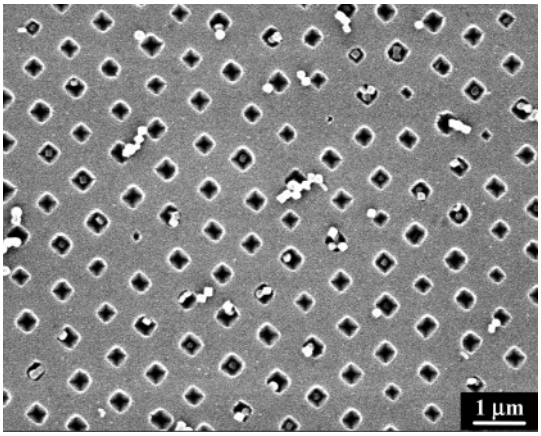

Figure 4. SEM image of particle precipitation on KOH etched silicon.

For longer etching duration, undercutting of silicon underneath the chromium nanoholes occurs. This leads to larger inverted pyramids (Figure 3B) with well-defined square bases. For shorter etching time (see Figure 3A), the corners of the square bases are not as sharp as those of over-etched ones. We also notice that there are some rectangular shaped pyramids in the anisotropic etched samples that are replicated from noncircular (e.g., oblate) nanoholes.[19] The size and depth of the inverted pyramidal pits can be easily controlled by adjusting the wet etching duration. Figure 3C shows the dependence of the size of the pyramids vs different etching time at 60 °C. More than 100 pyramids are measured using SEM to arrive at the reported size and size distribution of each sample. If we rise the reaction temperature to 80 °C, which is commonly used in anisotropic etching of silicon for micromachining,[34] the etching reaction becomes so vigorous that the precise control over the dimensions of the pyramids is more difficult.

For certain KOH etched samples, we find unwanted particle precipitation on the surface of the silicon wafer as well as in the pyramidal pits. Figure 4 shows a typical SEM image of such particles precipitated on an anisotropically etched n-type silicon wafer. Though these particles are sparsely distributed on the wafer surface, they affect the uniformity of the resulting gold nanopyramid arrays by creating random defects in the pyramids. Previous study shows that these particles are iron oxide precipitated from the reaction of iron impurities in KOH pellets with hydroxide ions.[35] A brief etching (1 min) in 2 M HCl aqueous solution at room temperature can easily remove these unwanted particles.[35]

(34) Madou, M. J. *Fundamentals of Microfabrication: the Science of Miniaturization*, 2nd ed.; CRC Press: Boca Raton, FL, 2002.

(35) Nielsen, C. B.; Christensen, C.; Pedersen, C.; Thomsen, E. V. *J. Electrochem. Soc.* **2004**, *151*, G338.

We then use the inverted silicon pyramids as the third generation templates to replicate metallic nanopyramid arrays. Conventional PVD deposition is carried out to deposit various metals in the silicon pits and form continuous metal films on the surface of the silicon wafer. For metals with weak adhesion to silicon, such as Au, Ag, Pt, and Pd, the deposited films can be adhered onto a glass substrate using a thin layer of polyurethane adhesive, followed by peeling off the silicon templates.[30] The resulting wafer-scale nanopyramid arrays exhibit striking diffractive colors and a characteristic six-arm diffractive star (Figure 5A). The adjacent arms of the diffraction star form exact 60° angles, a result indicating the formation of long-range hexagonal ordering.[27,36,37] Figure 5B shows a typical top-view SEM image of a replicated Au nanopyramid array. The hexagonal ordering of nanopyramids is clearly evident from the image. However, the periodic nanopyramids are polycrystalline, as is clear from the SEM images. The typical domain size is several hundred micrometers, limited by the single-crystal domain sizes of the original spin-coated monolayer colloidal crystal. Our previous results show that spin-coated monolayer crystals have much smaller single-crystal domains than multilayer crystals made by the same spin-coating process.[28] The gold pyramids are faithful replica of the original inverted silicon templates, indicating that no breaking of sharp tips occurred during the film peeling off procedure. Most of the pyramids have sub-10 nm sharp tips revealed by the magnified SEM image shown in the insets of images B and C in Figure 5 and the side-view SEM image in Figure 5C. The spacing between neighboring nanopyramids measured using SEM is the same as the original non-close-packed colloidal arrays. By a simple geometrical calculation, we estimate the nanotip density is about 6×10^8 tips cm^{-2} for 300 nm templating silica spheres. For metals with strong adhesion to silicon, such as Cr, Ni, and Al, the surface of silicon pits can be modified by octadecyl silane (ODS) to reduce the metal adhesion and facilitate the film peeling,[38] or a thin film of Au can be predeposited as a sacrificial layer before the deposition of adhesive metals. KOH/IPA wet etching can also be used to dissolve the silicon templates to release the metallic nanopyramid arrays provided the metals can survive the chemical etching.[19]

We evaluate the performance of our gold nanopyramid arrays as SERS substrates using benzenethiol as a model compound (Figure 6). In addition to the excellent affinity to gold surfaces, benzenethiol molecules have a large Raman cross-section, presumably as a result of chemical enhancement alongside electromagnetic enhancement.[2] The templated gold nanopyramid array sample (red curve) gives a strong Raman signal of adsorbed benzenethiol molecules. The positions of Raman peaks agree well with those in the literature for benzenethiol on gold substrates.[2,39,40] In control experiments, no SERS spectra are observed for benzenethiol molecules adsorbed on the flat sputtered gold films deposited under the same conditions on glass substrates (blue curve). The SERS enhancement factor for the gold nanopyramid substrate is estimated to be $\sim 7 \times 10^5$ using the method described in the literature by comparing the Raman intensity for two peaks at 1080 and 1581 cm^{-1}.[39,40] Previous results show that the greatest SERS enhancements occur when localized plasmon resonances on the structured metallic surfaces are present at both the excitation wavelength and Raman scattered wavelength.[40] Here the structural parameters

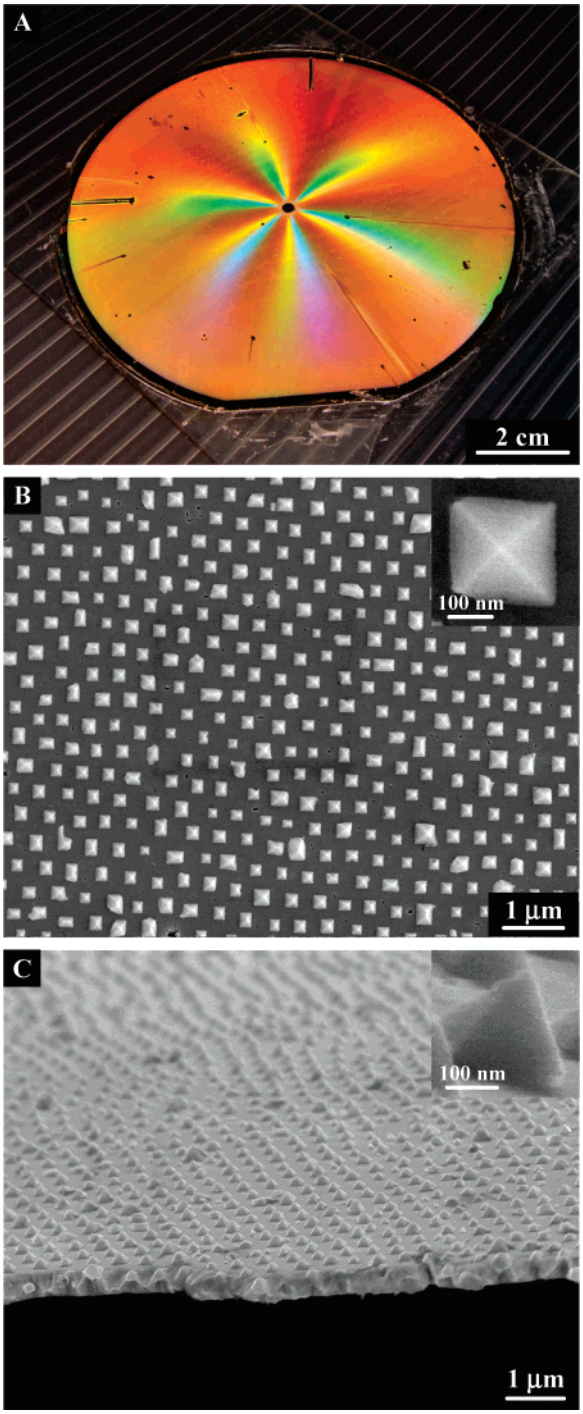

Figure 5. Periodic gold nanopyramid array. (A) Photograph of a 4 in. gold nanopyramid array templated from 320 nm silica spheres illuminated with white light. (B) Top-view SEM image of a replicated gold nanopyramid array. The inset showing a magnified SEM image of a single nanopyramid. (C) Side-view SEM image of the same gold nanopyramid array as in (B). A magnified pyramid is shown in the inset.

(36) Hoffman, R. L. *Trans. Soc. Rheol.* **1972**, *16*, 155.
(37) Pieranski, P. *Contemp. Phys.* **1983**, *24*, 25.
(38) Resch, R.; Meltzer, S.; Vallant, T.; Hoffmann, H.; Koel, B. E.; Madhukar, A.; Requicha, A. A. G.; Will, P. *Langmuir* **2001**, *17*, 5666.
(39) Abdelsalam, M. E.; Mahajan, S.; Bartlett, P. N.; Baumberg, J. J.; Russell, A. E. *J. Am. Chem. Soc.* **2007**, *129*, 7399.
(40) Cintra, S.; Abdelsalam, M. E.; Bartlett, P. N.; Baumberg, J. J.; Kelf, T. A.; Sugawara, Y.; Russell, A. E. *Faraday Discuss.* **2006**, *132*, 191.

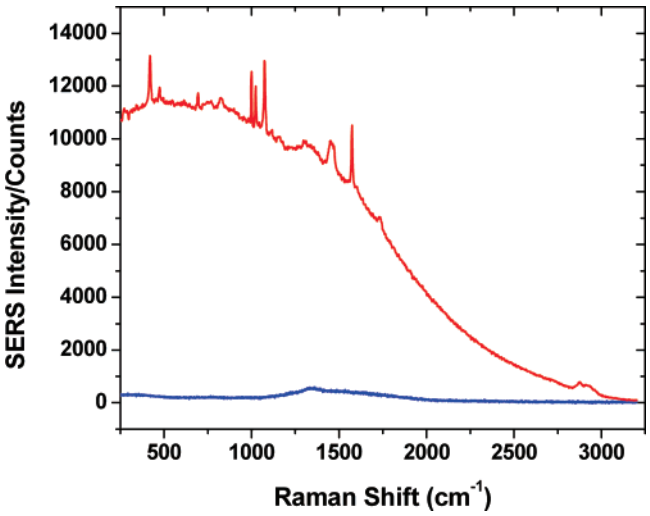

Figure 6. Raman spectra of benzenethiol adsorbed on a gold nanopyramid array (red curve) replicated from a silicon inverted pyramid array that is templated from 320 nm silica spheres and etched at 60 °C for 210 s and a flat gold control sample (blue curve).

of the gold nanopyramid arrays (e.g., pyramid size, separation, and height), which greatly affect the plasmon resonances, have not been optimized yet. We believe the SERS enhancement factor of our periodic substrates can be further improved by tailoring the structures of the templated nanopyramid arrays to match the optimal SERS requirements.

Conclusions

In conclusion, we have developed a simple templating approach for fabricating wafer-scale, periodic metallic nanopyramid arrays with nanoscale tips and high tip density. The size, depth, and separation of replicated nanopyramids can be easily controlled by changing the sizes of the templating silica spheres and the anisotropic KOH etching conditions. The adhesive peeling procedure allows for the reuse of silicon templates for making multiple replicas. Though this technique is simply based on self-assembly and templated fabrication, it is scalable and compatible with standard microfabrication, enabling the mass production of metallic nanostructures that are promising for applications in SERS substrates,[3] field-emission displays,[41] efficient OLEDs,[42] and surface plasmon devices.[4]

Acknowledgment. This work was supported in part by the start-up funds from the University of Florida, the UF Research Opportunity Incentive Seed Fund, and NSF Grant CBET-0651780. We thank Dr. Georgios Pyrgiotakis for his technical support on SERS measurements.

CM0712319

(41) Spindt, C. A.; Brodie, I.; Humphrey, L.; Westerberg, E. R. *J. Appl. Phys.* **1976**, *47*, 5248.
(42) Ichikawa, H.; Baba, T. *Appl. Phys. Lett.* **2004**, *84*, 457.